Geophys. J. Int. (1996) **127**, 339–347

Experiments on Joule heating and the dissipation of energy in the Earth's core

Daniel Brito,[1,*] Philippe Cardin,[1] Henri-Claude Nataf[1] and Peter Olson[2]

[1] *Département Terre Atmosphère Océan, École Normale Supérieure, URA 1316 du CNRS, 24, rue Lhomond, 75231 Paris Cedex 05, France*
[2] *Earth and Planetary Sciences, Johns Hopkins University, Baltimore MD 21218, USA*

Accepted 1996 June 19. Received 1996 May 29; in original form 1996 March 18

SUMMARY

We present measurements of Joule heat production in a fluid gallium vortex permeated by a uniform transverse magnetic field. We find that the Joule heat production increases as the square of the imposed field intensity for weak and moderately strong magnetic fields and magnetic Reynolds numbers up to about one. For stronger magnetic fields, Lorentz forces destroy the 2-D structure of the vortex and the Joule heat production becomes nearly independent of the intensity of the imposed magnetic field. We derive scaling laws relating fluid velocity in the vortex, imposed magnetic field intensity and Joule heat production, for both low and high magnetic Reynolds number regimes. Application of these laws to magnetic induction in the Earth's fluid core indicates that Joule heat production by this mechanism is large enough to limit the intensity of magnetic fields within the core.

RÉSUMÉ

Dans cet article, nous présentons des mesures de puissance de dissipation ohmique (effet Joule) effectuées dans un vortex de gallium soumis à un champ magnétique uniforme transversal. Nous trouvons que la production de chaleur est proportionnelle au carré de l'intensité du champ magnétique appliqué, pour des champs faibles et modérés, et pour un nombre de Reynolds magnétique inférieur à 1. Pour des champs plus forts, les forces de Laplace détruisent la bidimensionalité du vortex, et la production de chaleur par effet Joule devient pratiquement indépendante de l'intensité du champ magnétique appliqué. Nous établissons des lois d'échelles qui relient la vitesse du fluide dans le vortex, l'intensité du champ magnétique appliqué, et la puissance ohmique dissipée, pour les régimes à bas et haut nombre de Reynolds magnétique. L'application de ces lois à l'induction magnétique dans le noyau terrestre indique que la production de chaleur par ce mécanisme est assez grande pour limiter l'intensité du champ magnétique dans le noyau.

Key words: Earth's core, Earth's magnetic field, geodynamo, heat flow.

1 INTRODUCTION

The geomagnetic field is continually regenerated by motions of the electrically conducting iron-rich outer core. Although the concept of a self-sustaining dynamo is widely accepted for the core (Elsasser 1946; Bullard & Gellman 1954; Loper & Roberts 1983; Braginski 1990; Cardin & Olson 1992), many of the critical parameters are unresolved. For example the intensity of the magnetic field on the core–mantle boundary is known to be about 0.5 mT (Voorhies 1986; Bloxham, Gubbins & Jackson 1989), but inside the electrically conducting core the field intensity is essentially unknown. Some dynamo theories predict intense toroidal fields in the core, of the order 1000 mT (Kumar & Roberts 1975; Braginski 1990), whereas other theories predict the core toroidal field is only about as strong as the dipole field (Pekeris, Accad & Shkoller 1973; Busse, 1975). The Glatzmaier & Roberts (1995) numerical simulation of thermal convection in a rotating, electrically conducting fluid sphere produced an external magnetic field with an amplitude similar to the Earth's dipolar field with an internal field of the order 10 mT. Zhang & Fearn (1993) have

* Email: brito@geophy.ens.fr

argued that diffusive instabilities limit the strength of the toroidal field to about 10 mT or less. It is clear from the spread of values among these estimates that the toroidal field is very poorly constrained despite the fact that its value would dramatically change our understanding of the dynamo.

Another important but poorly understood process is the mechanism by which the dynamo dissipates energy. It is generally agreed that the kinetic energy in the core is transformed into heat primarily by Ohmic, rather than viscous, dissipation (Verhoogen 1980). The rate of Ohmic dissipation is the Joule heat production, given by

$$P_J = \int_{\text{core}} \frac{\mathbf{J}\cdot\mathbf{J}}{\sigma}\, dV, \tag{1}$$

where $\mathbf{J}$ is the current density and σ is the electrical conductivity. Since

$$\mu_0 \mathbf{J} = \nabla \times \mathbf{B}, \tag{2}$$

where $\mathbf{B}$ is the magnetic induction, the process of energy dissipation is closely related to the intensity and the structure of the magnetic field in the core.

Theoretical considerations indicate the dynamo is dissipation-limited, which implies there is a close relationship between the energy available to drive the dynamo and the energy dissipated by the dynamo. For example, in convection-driven dynamos the dissipation is proportional to the convective heat transport P_C via

$$P_J = \eta P_C, \tag{3}$$

where $\eta \simeq 0.1$ is the thermodynamic efficiency factor. Since the core energy budget limits the convective heat transport to roughly $P_C \leq 5$ TW (Verhoogen 1980; Lister & Buffett 1995), the Joule heat production is limited to about $P_J \leq 0.5$ TW.

The amount of Joule heating associated with the present-day dipole moment of the geomagnetic field is only about 10^{-2} TW, well below the thermodynamic limit. However, it is likely that Joule heating in the core is concentrated in smaller-scale current systems that do not contribute directly to the dipole moment (Gubbins, Masters & Jacobs 1979). Evidence for dissipation in smaller-scale electrical currents comes from the spectrum of the geomagnetic field on the core–mantle boundary (CMB). Excluding the dipole term, the power spectrum of the radial field on the CMB is nearly constant out to spherical harmonic degree $l = 13$, the limit of resolution of the core field (Hulot & Le Mouël 1994). Since the magnetic energy spectrum is nearly constant, the energy dissipation spectrum may actually *increase with spherical harmonic degree* over this range, implying that Joule heating is larger at higher degrees, that is, at short length scales.

The experiments we present here illustrate this effect, demonstrating that the Joule heating occurs on the internal length scales of the flow, in particular on the scale of vortices. We measure the dissipation in a fluid vortex permeated by a transverse magnetic field. This serves as a simplified model for dissipation in the core: the vortex represents a single geostrophic convection column with its axis parallel with the axis of rotation (Busse 1970; Cardin & Olson 1994; Brito *et al.* 1995) and the transverse magnetic field represents the toroidal magnetic field in the core.

A previous study (Brito *et al.* 1995) examined the dynamics of a mechanically driven geostrophic vortex of gallium in a transverse magnetic field. In that study, the effect of the Lorentz force on the circulation and radius of the vortex was determined, and the pattern of the induced magnetic field was delineated.

Here, we use the same apparatus to measure the Joule heating that results from the interaction of the vortex and the imposed magnetic field. The experimental results, up to a magnetic Reynolds number of 0.3, are compared with two simplified theoretical models of Joule heating, valid at low and high magnetic Reynolds numbers and then extrapolated to the parameter regime of the Earth's core.

The layout of this paper is as follows. We describe the design of the experiment in Section 2, and the Joule heating results are given in Section 3. A simple scaling law for these results is derived in Section 4, together with an analytical extension of this law for very large magnetic Reynolds numbers. In Section 5, we extrapolate our results to estimate the dissipation in the Earth's core. Conclusions and perspectives are presented in Section 6.

2 EXPERIMENTAL APPROACH

2.1 Experimental set-up

The experimental set-up is essentially the same as in Brito *et al.* (1995), hereafter referred to as Paper I. Fig. 1 illustrates the main features. A polycarbonate cylinder [8 cm (inner diameter) × 22 cm (inner height)] is filled with liquid gallium (one litre) and is mounted vertically between the poles of an electromagnet. The physical properties of gallium required for the analysis are listed in Table 1 (Pascal 1961). The magnet

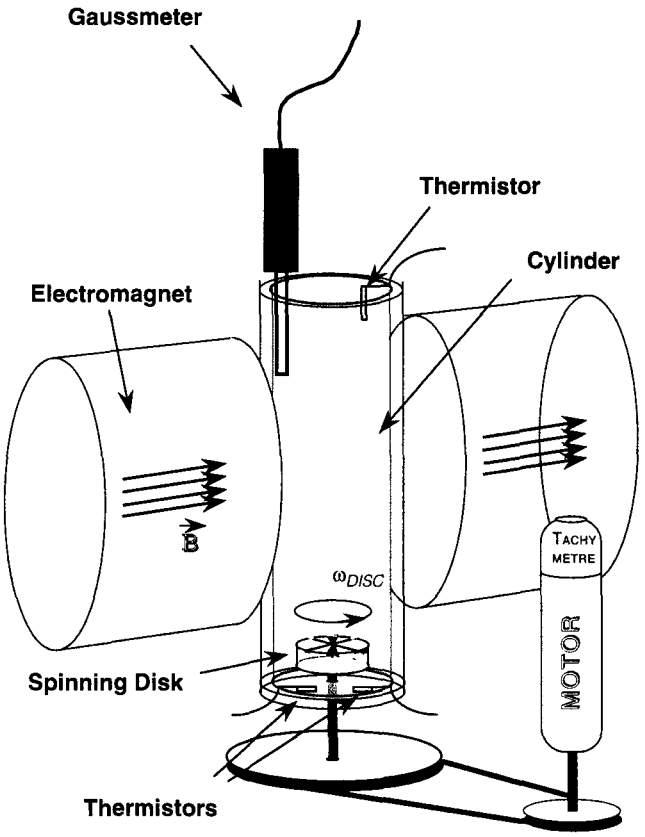

Figure 1. Sketch of the experimental set-up.

Table 1. Physical properties of liquid gallium (Pascal 1961).

Density	ρ	$kg\,m^{-3}$	6.09×10^3
Kinematic viscosity	ν	$m^2\,s^{-1}$	3.1×10^{-7}
Electrical conductivity	σ	$(m\Omega)^{-1}$	3.68×10^6
Melting point	T_m	°C	29
Boiling point	T_b	°C	2227
Coefficient of thermal expansion	α	K^{-1}	1.0×10^{-4}
Surface tension	γ	$N\,m^{-1}$	0.735
Specific heat	C	$J\,kg^{-1}\,K^{-1}$	410

produces a uniform horizontal magnetic field between the two 16 cm diameter poles with a maximum intensity of 80 mT. The magnet axis passes 13 cm above the base of the cylinder.

A fluid vortex with a vertical axis is created in the gallium by the steady rotation of a 4 cm diameter crenellated disc, located 3.8 cm above the base of the cylinder. The disc is connected to a speed- and torque-controlled motor, via a shaft and drive-belt system. The motor is shielded from the fluid in order to avoid interference with the applied or induced magnetic fields.

Temperature in the fluid is recorded by a thermistor located near the top of the cylinder, as shown in Fig. 1. Two other thermistors located in the polycarbonate base plate are used to monitor the effects of friction at the rotary joint where the motor shaft enters the cylinder. In addition to measuring temperature, we also measure the horizontal component of the induced field, in the direction perpendicular to the applied field, using a Gaussmeter positioned just outside the polycarbonate cylinder, at a height of 13 cm above its base.

There are several differences between the set-up of this experiment and the experiment reported in Paper I. Among these are: (1) the cylinder and applied magnetic field are at rest in the laboratory frame, whereas they were rotating in Paper I; (2) in this experiment we use disc velocities up to 1500 rev min^{-1}, whereas velocities less than 600 rev min^{-1} were used in Paper I; and (3) the top cover that received an array of Venturi tubes in Paper I is replaced by a plain cover with a Pt-100 thermistor (3 mK precision) attached to it.

2.2 Measurement of heat production in liquid gallium

The principle of our experiments is very simple: we measure the heat production from dissipative processes in the fluid by monitoring the increase in temperature of the liquid gallium as a function of time. If the cylinder was perfectly insulated and Joule heating the only source of dissipation, we would have

$$P_J = mC\frac{d\bar{T}}{dt}, \tag{4}$$

where P_J is Joule power, m is the mass of fluid, C is the specific heat and $\bar{T}$ is the average temperature of gallium. In reality, the experiment involves additional sources of heat and the polycarbonate container is not perfectly insulating. The most important complicating effects consist of heat loss, P_{loss}, through the insulated walls of the cylinder, heat production by viscous dissipation in the liquid, P_μ, and frictional heating by the shaft of the spinning disc, P_{shaft}. Including these effects leads to

$$mC\frac{d\bar{T}}{dt} = P_J + P_\mu + P_{shaft} - P_{loss}. \tag{5}$$

We estimated the relative importance of each of these effects using a series of preliminary tests of the device. The dominant heat source turns out to be P_{shaft}, which is typically a factor of 10 larger than the dissipation within the fluid.

In order to eliminate the contribution of P_{shaft} and P_{loss} in (5), we use *differential* measurements of temperature increase, as follows. Prior to and during each experiment, the cylinder is maintained at a temperature of about 40 °C by a circulating hot-air system. To begin each experiment, the disc is spun from rest to a constant angular velocity ω_{disc} and maintained at this velocity until the temperature near the shaft (measured by the two auxiliary thermistors shown in Fig. 1) is 2 °C higher than the temperature in the gallium. We then switch on the electromagnet, applying a steady magnetic field with intensity $B_{imposed}$ and record the fluid temperature at 10 s intervals for about 3 min. We then switch off the electromagnet and continue recording temperature for another 3 min, again at 10 s intervals.

Since the liquid is well stirred by the swirling vortex, the temperature measured at the top approximates very closely the average temperature of the gallium. Using the *difference* in the rate of temperature increase with and without the magnetic field eliminates the contribution from P_{shaft}. It also largely eliminates the contribution to (5) from imperfect insulation, since P_{loss} is proportional to the temperature difference between the liquid and the outside temperature, which is almost constant during a complete run. Finally, viscous dissipation is found to be negligible compared with Ohmic dissipation, as anticipated (Tritton 1988). The characteristic spin-down time of the fluid is of the order of 10 s, which yields a maximum viscous dissipation of about 0.6 W.

Fig. 2 shows a typical record of temperature in the fluid obtained using this technique. The temperature–time-series is piecewise linear, with a clear decrease in slope when the

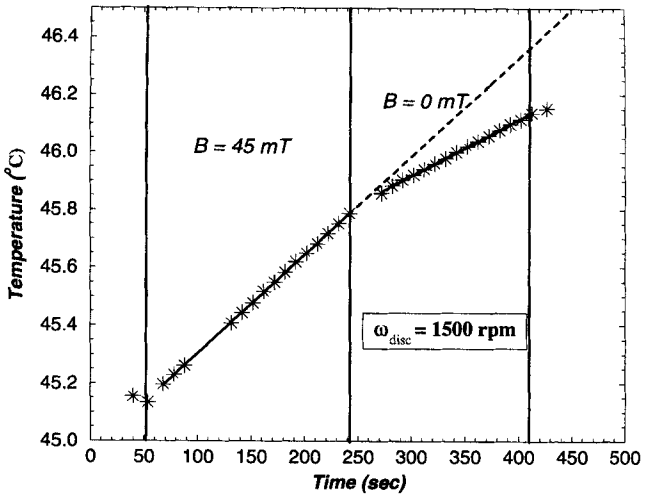

Figure 2. Temperature increase measured for $\omega_{disc} = 1500$ rev min^{-1}. From 50 s to 250 s a magnetic field of 45 mT is applied, and from 250 s to 410 s the electromagnet is switched off. Each asterisk (every 10 s) is one measurement of the temperature at the top of the vortex. The lines are the least-squares fits for $(dT/dt)^{B=45}_{\omega=1500}$ and $(dT/dt)^{B=0}_{\omega=1500}$ of eq. (6). Notice the difference in slope between the dashed line and the solid line during the second part of the experiment (after 250 s): the increase of temperature in the tank of gallium is larger when the magnetic field is applied because of the heat dissipated by the electrical currents (Joule heating).

magnetic field is switched off. According to the arguments given above, the difference in slope yields the Joule heating P_J as a function of ω_{disc} and B_{imposed} as follows:

$$P_J = mC\left[\left(\frac{dT}{dt}\right)^{B=B_{\text{imposed}}}_{\omega=\omega_{\text{disc}}} - \left(\frac{dT}{dt}\right)^{B=0}_{\omega=\omega_{\text{disc}}}\right]. \quad (6)$$

In evaluating the right-hand side of this expression, we determine the slopes of the two segments of dT/dt using the least-squares fits of linear equations to the data points, and then compute the difference in the two slopes. To verify that the break in slope with change in magnetic field was repeatable, we carried out preliminary tests where the magnetic field was switched on and off several times. We observed repeated slope changes similar to those in Fig. 2.

3 EXPERIMENTAL RESULTS

3.1 Joule heating

Joule heating was measured with the techniques described above for disc velocities ω_{disc} of 600, 1000, 1250 and 1500 rev min^{-1}, and applied magnetic fields from 0 to 80 mT. Fig. 3 displays the results. The error bars are the 2σ standard deviations deduced from the linear fits to the temperature–time-series only. The data points for $\omega_{\text{disc}} = 1500$ rev min^{-1} illustrate the behaviour we find generally. These data exhibit two regimes. In the first regime, for magnetic fields up to about 40 mT, Joule heating increases nearly quadratically with the field intensity. Beyond this value is a second regime where Joule heating levels off and perhaps even decreases with increasing field strength. For lower values of ω_{disc}, similar behaviour is seen, except that the transition between the two regimes occurs at a correspondingly lower value of magnetic field.

The existence of two regimes in Joule heating is consistent with the experimental findings in Paper I. In Paper I, measurements of pressure profiles at the top of the vortex, electrical potentials and the induced magnetic field identified two distinct flow regimes. In those experiments the controlling parameter was found to be the Elsasser number, the ratio of Lorentz to Coriolis forces. It was observed that for a low Elsasser number, less than approximately 0.2 (corresponding to low imposed magnetic fields), the vortex is slowed down by the magnetic field but remains essentially 2-D and extends throughout the height of the cylinder. The effective diameter of the vortex increases with the imposed field in this regime. At higher values of the imposed field (or, alternatively, smaller values of Ω_{Table}), corresponding to larger Elsasser numbers, the vortex is nearly arrested by the magnetic field, and the basic two-dimensionality of the flow is destroyed. For increasing field strengths, the motion in the fluid is increasingly confined to the vicinity of the spinning disc in this regime. Nevertheless, the fluid always seems well mixed because we see an immediate response in the temperature to changes in the field strength, for both increasing and decreasing field strengths.

In Section 4 we will present a quantitative analysis of our results on Joule heating in terms of the vortex velocity, and demonstrate that the transition between these two flow regimes explains the Joule heating data.

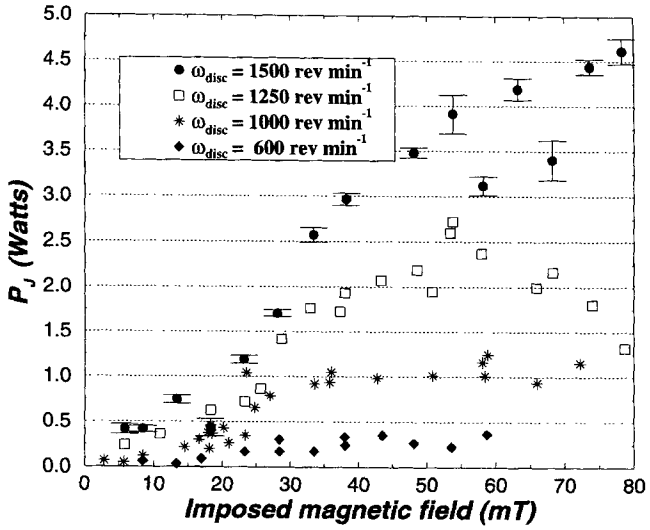

Figure 3. Joule heating measured for $\omega_{\text{disc}} = 600$, 1000, 1250 and 1500 rev min^{-1}. We clearly observe two regimes for the four different velocities. The second regime is reached for a lower magnetic field when the velocity of the disc is lower. Note that error bars are the 2σ standard deviation deduced from the linear fits to the temperature–time-series only.

3.2 Torque measurements

In addition to measuring the heat dissipated within the fluid, we monitored the torque applied by the motor that drives the disc. Torque variations were recorded as a function of time in all the experiments. Using the same differential measurement technique as described above for heating, we have obtained the torque Γ_L applied by the fluid on the disc when Lorentz forces are present. A simple energy balance indicates that Ohmic dissipation within the fluid is equal to the work done on the fluid by Lorentz forces, and is thus related to the torque driving the disc by

$$P_J = \Delta\Gamma_L \omega_{\text{disc}}, \quad (7)$$

where $\Delta\Gamma_L$ is the torque difference between the portions of the experiment with and without the field of the electromagnet imposed. In principle, this provides an alternative measurement of Joule heating. We find that the dissipation measured this way depends on the field intensity in the same way as the measurements shown in Fig. 3, except for one important difference. The dissipation derived from the torque is always about 3.5 times larger than that obtained from the temperature-series. We could not find the reason for this systematic discrepancy, but because they are more direct, we regard the temperature measurements as being more accurate.

3.3 Induced magnetic field

Fig. 4 shows the ratio of the induced magnetic field to the imposed field, as a function of the imposed field intensity, for several disc velocities. The two regimes are clearly identified. In the low-field regime the efficiency of the induction decreases slowly as the magnetic field is increased up to $B_{\text{imposed}} \simeq 40$ mT, as a consequence of the decrease in vortex velocity. At values of $B_{\text{imposed}} > 40$ mT, the ratio decreases sharply with increasing imposed field as the vortex looses its two-dimensionality.

Accordingly, for each regime and each velocity of the disc,

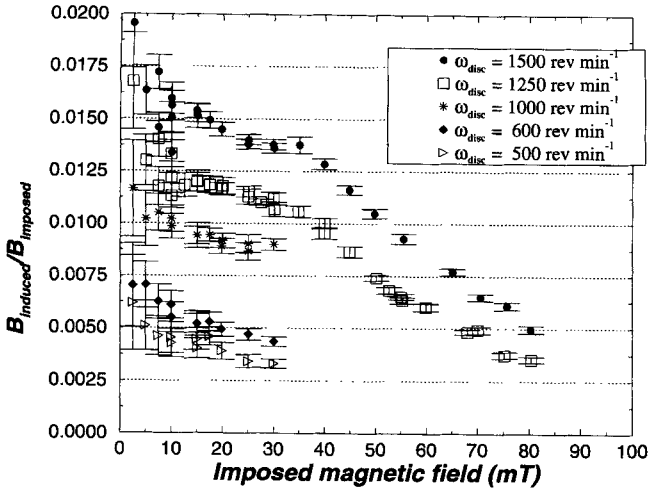

Figure 4. Induced magnetic field measured outside the cylinder during the experiments for different imposed magnetic fields from 2.5 mT to 78 mT, and for different velocities of the disc. The ratio $B_{induced}/B_{imposed}$ increases with the velocity of the disc. Note the break of slope for $\omega_{disc} = 1250$ and 1500 rev min^{-1} around 35–40 mT.

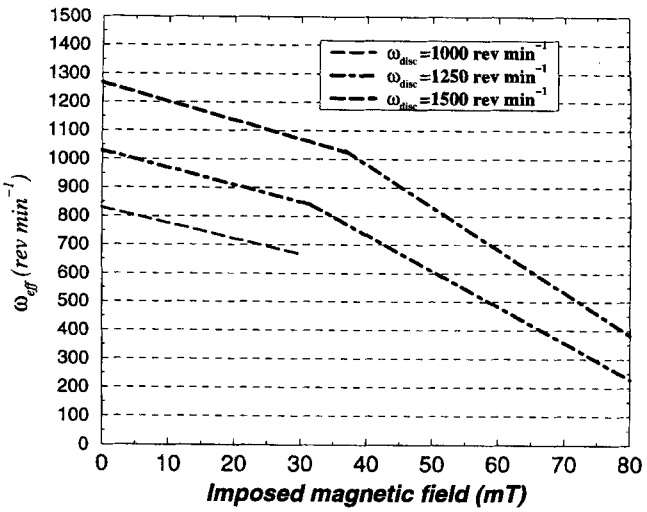

Figure 5. Effective angular velocity in the vortex as a function of the imposed magnetic field, $\omega_{eff}(B) = [U_{eff}(B)]/R$, obtained from the measurements of the induced magnetic field. Note that for zero imposed magnetic field, the velocity at the top of the vortex is slightly lower than the velocity of the disc, demonstrating that the vortex is not completely 2-D.

we fit the data by a linear function of $B_{imposed}$:

$$B_{induced}/B_{imposed} = A_0 + A_1 B, \tag{8}$$

where the two constants A_0 and A_1 are obtained from the linear fits of the data of Fig. 4. It was demonstrated in Paper I that the ratio $B_{induced}/B_{imposed}$ is proportional to the effective magnetic Reynolds number, $Re_m = \mu_0 \sigma U_{eff} R$, where σ is the electrical conductivity, μ_0 the magnetic permeability, R a typical dimension (here the disc radius), and U_{eff} the typical effective velocity (here $\omega_{eff} R$). We expect this relationship to remain valid over the parameter regime of this experiment as well. Thus, we have a second relationship:

$$B_{induced}/B_{imposed} = C_1 Re_m = C_1 \mu_0 \sigma R U(B), \tag{9}$$

where $C_1 = 6.61 \times 10^{-2}$ from Paper I.

Accordingly, we use these last two relationships (8) and (9) between $B_{induced}/B_{imposed}$ and Re_m to deduce the vortex velocity U_{eff}. Fig. 5 shows the results in terms of effective angular velocity $\omega_{eff} = U_{eff}(B)/R$ as a function of the imposed magnetic field $B_{imposed}$.

4 INTERPRETATION OF THE RESULTS

We wish to find a simple relationship between the amount of Joule heating, the fluid velocity in the vortex, and the intensity of the imposed field. Simple physical considerations suggest a relationship of the form

$$P_J = a\sigma U^2 B^2, \tag{10}$$

where a is a constant which depends on geometry, σ is the electrical conductivity, U is the typical velocity, and B the typical magnetic field. This scaling can be obtained by combining the relationship between the current density J and the electromotive force,

$$J \simeq \sigma U B, \tag{11}$$

and the definition of Joule heating,

$$P_J = \int_V \frac{J^2}{\sigma} dV. \tag{12}$$

The main assumption underlying (10) is that the magnetic Reynolds number of the flow is small, implying $B_{induced} \ll B_{imposed}$. This is certainly the case in the experiment, but is problematic in the core. Because of this ambiguity, we examine two models of Joule heating. The first is appropriate for small magnetic Reynolds numbers, which yields the scaling given in (10). The second model, appropriate for the limit of very large magnetic Reynolds numbers, yields a somewhat different scaling law. We then compare the predictions of each law for dissipation in the Earth's core.

4.1 Joule heating at low magnetic Reynolds number

In Paper I, we introduced a simple 2-D kinematic model of an MHD vortex, consisting of a core in a solid-body rotation plus a shear layer that adjusts the vorticity of the core to the vorticity of the container. There are only two parameters in this model, the radius R_{solid} of the vortex core, and its angular velocity ω_{solid}. In Paper I, we also computed the distribution of the Foucault electrical currents generated by this simple vortex in an imposed horizontal magnetic field, taking into account the finite vertical extent of the cylinder. Fig. 6 shows the distribution of Joule heating in the model, computed from the electrical currents. Joule heating mostly occurs along the loop of current close to $r = R_{solid}$, in the plane that contains $\mathbf{B}$, where the product $\mathbf{U} \times \mathbf{B}$ is maximum.

To obtain a scaling law between Joule heating and the other parameters, we will simplify the model further, by treating the vortex as if it were infinitely long and neglecting the $\nabla\varphi$ term in the expression for the current density,

$$\mathbf{J} = \sigma(\mathbf{U} \times \mathbf{B} - \nabla\varphi). \tag{13}$$

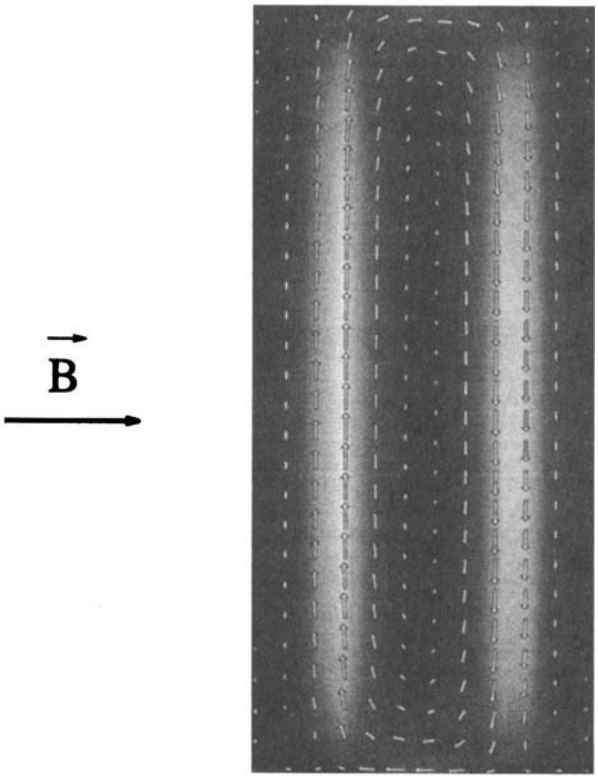

Figure 6. Numerical model of Foucault electrical currents in the cylinder. View of the vertical section of the cylinder that contains the imposed magnetic field **B**. **J** is represented by arrows. Foucault electrical currents consist of a loop of current with upward currents on the left and downward currents on the right. The grey areas are the distribution of the Joule heating in the cylinder: the brightest area (area of the largest dissipation) is located along the loop of current where $J \simeq \sigma UB$ is maximum. This model depends on two parameters, R_{solid} and ω_{solid}. R_{solid} is the radius of solid-body rotation and determines the geometrical distribution of the electrical currents. ω_{solid} is the angular velocity of the solid-body rotation, which controls the amplitude of the currents.

The Joule heating then becomes

$$P_J = \int_V \frac{J^2}{\sigma} dV = \int_V [\sigma \mathbf{U} \times \mathbf{B}]^2 r dr\, d\theta\, dz \tag{14}$$

$$= H \iint_S \sigma U^2(r) B^2 \cos^2\theta\, r dr\, d\theta . \tag{15}$$

Introducing $R_{solid} = fR_{vortex}$ (with $0 \le f \le 1$), and using the velocity distribution in Appendix A of Paper I, we get:

$$P_J = \sigma H \pi \left(\int_0^{fR_v} \omega^2 r^2 r dr + C \int_{fR_v}^{R_v} \left(\frac{R_v^2}{r} - r \right)^2 r dr \right), \tag{16}$$

where

$$C = \frac{\omega f^2}{1 - f^2}, \tag{17}$$

leading to

$$P_J = \sigma U(f)^2 B^2 V \times \underbrace{\left\{ \frac{f^2}{4} + \frac{f^2}{(1-f^2)^2} \left[-\frac{3}{4} - \frac{f^4}{4} + f^2 + \ln\left(\frac{1}{f}\right) \right] \right\}}_{C(f)}. \tag{18}$$

According to (18), Joule heating varies as $\sigma U^2 B^2$, where U is the actual velocity for a given imposed B. In our model, U and P_J also depend on the radius of solid-body rotation. If we take $R_{solid} = R_{disc} = 1/2 R_{vortex}$ (i.e. $f = 1/2$), as suggested by the results of Paper I, we obtain

$$P_J = 1.3 \times 10^{-4} \sigma U^2(B) B^2 \tag{19}$$

for the scaling law at low magnetic Reynolds number.

4.2 Joule heating in the experiments

The measurements in Section 3.1 show the variation of Joule heating as a function of the imposed magnetic field, for various disc velocities. We now compare these data with the scaling law derived in the previous section. In order to make this comparison, we must relate the measured Joule heating to the actual fluid velocity in the vortex. To obtain the fluid velocity, we use the induced magnetic field shown in Fig. 4 in conjunction with the calibration between the vortex velocity and the induced magnetic field derived in Paper I. In doing so, we implicitly neglect the effect of the small variation of the radius of solid-body rotation found in Paper I. In using this approach we are also implicitly assuming that the vortex remains 2-D. This assumption certainly breaks down for the highest values of the imposed magnetic field tested here. In addition, uncertainties on the position of the Gaussmeter as compared to its location in Paper I (about 2 mm) can result in errors in the induced field and velocity of about 20 per cent. With these approximations in mind, we proceed as follows. We first derive the velocity $U(B)$ by fitting two straight-line segments to the curves $B_{induced}/B_{imposed} = f(B_{imposed})$. One segment is for the first regime (up to $B_{imposed} = 30$ mT); the other one is for the regime where the induced field (and hence U) decreases more strongly. By comparing with the Joule heating measurements, we deduce the following experimental law:

$$P_J \simeq 1.4 \times 10^{-4} \sigma U^2(B) B^2 . \tag{20}$$

We note the remarkable consistency between this experimental law and the law (19) derived from the 2-D model. Fig. 7 compares the actual experimental results with the predictions of this law (20).

There is agreement in the first regime, where P_J is nearly quadratic in B. For higher values of B, our law predicts that Joule heating levels off and finally decreases with increasing B, in agreement with the set of measurements for $\omega_{disc} = 1250$ rev min^{-1}, but not so evident for other disc velocities. This drop in Joule heating, which is due to the strong reduction in fluid velocity by the magnetic field and strong departures from two-dimensionality in the vortex, is not as clear for the other values of the imposed disc velocity.

4.3 Joule heating at high magnetic Reynolds number

The maximum magnetic Reynolds number reached in our experiments is $Re_m \simeq 0.3$ and the previous analysis is probably valid up to this value. For application to the Earth's core, however, it is necessary to consider how the relationship

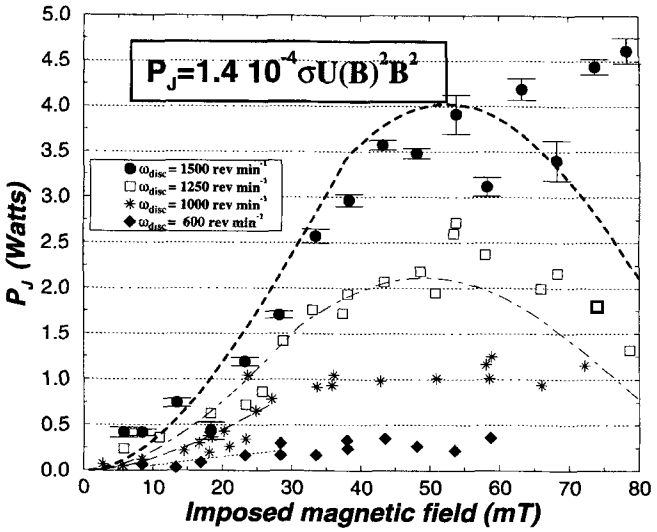

Figure 7. The dashed lines show fits of the experimental data set by a global scaling law for the Joule heating of the type $P_J = a\sigma U(B)^2 B^2$. $U(B)$ in this law is derived from the measurements of the induced magnetic field. The fit predicts the two regimes reasonably: at first, a quadratic increase of the Joule heating in U and B, and for the high applied magnetic fields, a slight decrease of the Joule heating linked to the break of the vertical rigidity of the vortex.

between Joule heating and imposed magnetic field changes at higher magnetic Reynolds numbers. Here we consider the limit of a high magnetic Reynolds number, the regime where advection of magnetic field dominates over diffusion. In this regime the classical law in $\sigma U^2(B) B^2_{\text{imposed}}$ breaks down because the imposed magnetic field strength is no longer representative of the magnetic field within the vortex.

To derive the appropriate law for this regime, we follow Roberts (Gubbins & Roberts 1987), who considers a uniform conductor filling the whole space, and everywhere at rest except for a cylindrical rotor of radius R_{rotor}, which spins about its vertical axis with an angular velocity ω. A uniform horizontal magnetic field B_{imposed} is applied. Roberts demonstrates that when $Re_m \gg 1$, the magnetic field is expelled from the interior of the rotor to form flux sheets near its surface.

This 2-D model is based on flux expulsion, at large Re_m. In this regime, the breakdown of 2-D structures seen in Paper I at $\Lambda \simeq 0.2$ may occur at larger Elsasser numbers values. Indeed, numerical experiments of magnetoconvection (Olson & Glatzmaier 1995) show breakdown of 2-D structures for $\Lambda \geq 1$.

Roberts derived the analytical expression of the total magnetic field ($\mathbf{B}_2$) just outside the rotor, as a function of B_{imposed}, in the limit $Re_m \to \infty$. Note that in this limit the interior magnetic field $\mathbf{B}_1$ is zero.

For finite Re_m, the discontinuity of B will be smoothed on a length scale $\delta = \sqrt{2/(\mu_0 \sigma \omega)}$ called the skin. The tangential components of the magnetic field are related to the surface electrical current $\mathbf{J}_s$, which develops on the surface of the rotor, by

$$\mathbf{B}_1^T - \mathbf{B}_2^T = \mu_0 (\mathbf{J}_s \times \mathbf{n}_{12}), \tag{21}$$

where $\mathbf{n}_{12}$ is the unit vector perpendicular to the rotor. Since the interior magnetic field $\mathbf{B}_1$ is zero, we deduce $\mathbf{J}_s$ from the expression of $\mathbf{B}_2^T$ given by Roberts (Gubbins & Roberts 1987). Integrating $\mathbf{J}_s^2$ along the rotor and over its height H_{rotor}, we get the expression for Joule heating:

$$P_{\text{Jrotor}} = \frac{4\pi B^2 R_{\text{rotor}} H_{\text{rotor}}}{\mu_0^2 \sigma \delta}, \tag{22}$$

$$P_{\text{Jrotor}} = \frac{2\sqrt{2}\pi B^2 R_{\text{rotor}} H_{\text{rotor}} \sqrt{\omega}}{\mu_0^{3/2} \sigma^{1/2}}. \tag{23}$$

Rewriting this in terms of the magnetic Reynolds number, we get:

$$P_{\text{Jrotor}} = 8.89 H_{\text{rotor}} B^2 \frac{\sqrt{Re_m}}{\mu_0^2 \sigma}. \tag{24}$$

4.4 Ohmic dissipation as a function of the magnetic Reynolds number

The expression for Joule heating as a function of the actual fluid velocity in our experiments, rewritten in terms of the actual magnetic Reynolds number, is

$$P_J = 1.56 \times 10^{-1} \pi R_{\text{vortex}}^2 H_{\text{vortex}} B^2 \frac{Re_m^2}{\mu_0^2 \sigma \dfrac{R_{\text{vortex}}^2}{4}}$$

or

$$P_J = 1.96 H_{\text{vortex}} B^2 \frac{Re_m^2}{\mu_0^2 \sigma}, \tag{25}$$

and is valid for low magnetic Reynolds numbers. For high magnetic Reynolds numbers we obtained the following expression:

$$P_J = 8.89 H_{\text{vortex}} B^2 \frac{\sqrt{Re_m}}{\mu_0^2 \sigma}. \tag{26}$$

Fig. 8 represents $P_J(2\mu_0^2 \sigma / HB^2)$ as a function of Re_m. The laws corresponding to the two different Re_m regimes are shown, together with our experimental data points.

5 APPLICATION OF JOULE HEATING IN THE EARTH'S CORE

Formula (3) for dynamo efficiency from the Introduction is rewritten in terms of core heat loss,

$$P_{\text{Jcore}} = \eta P_{\text{CMB}}, \tag{27}$$

where P_{Jcore} is Joule heat production in the Earth's core, P_{CMB} is the total heat flowing out of the core, and η is an efficiency factor. There is a considerable uncertainty in both η and P_{CMB}, but reasonable upper bounds seem to be:

$$\eta \leq 0.10, \tag{28}$$

$$P_{\text{CMB}} \leq 5TW \tag{29}$$

(Lister & Buffett 1995), from which we get

$$P_{\text{Jcore}} \leq 0.5TW. \tag{30}$$

This upper bound has often be used in the framework of kinematic dynamos to check the viability of the dynamo and to put an upper bound on the intensity of the toroidal magnetic field in the core. Indeed, only the radial component of the poloidal part of the Earth's magnetic field can be obtained from measurements at the surface. Its maximum intensity at the surface of the core is about 0.5 mT. However, the constraint

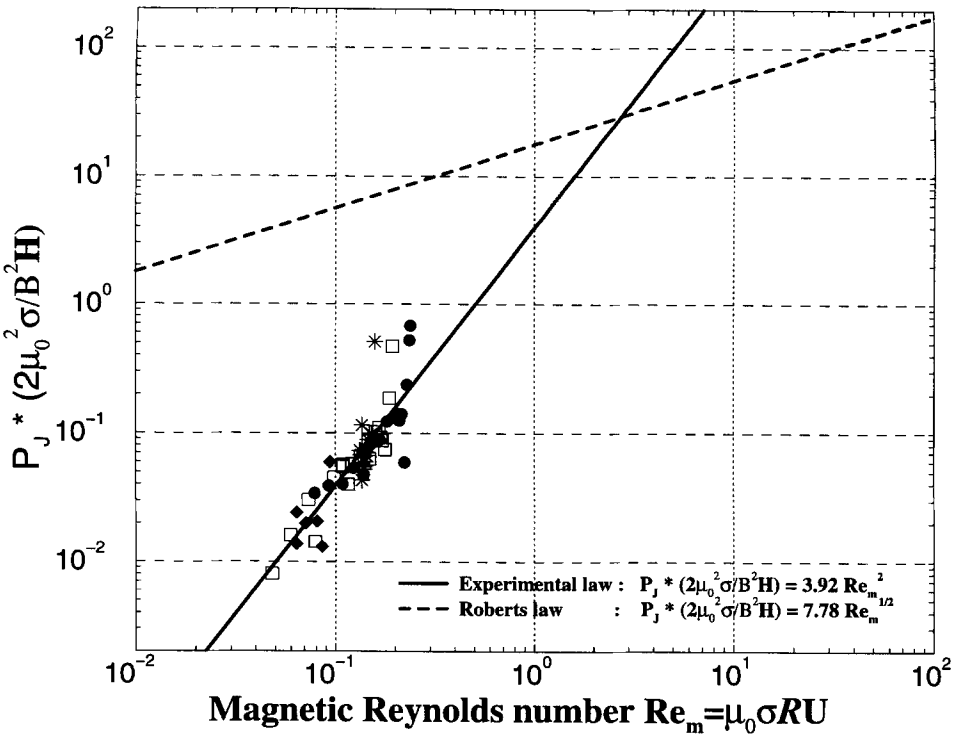

Figure 8. P_J is the total Joule heating (W) dissipated in a vortex and is scaled by a typical power (magnetic energy divided by magnetic diffusion time); σ is the electrical conductivity of the fluid, H is the height of the vortex and B is the transverse magnetic field applied. The characteristic length scale used for the magnetic Reynolds numbers is the radius of the vortex, and the characteristic velocity scale is the $U=\omega R$, where ω is the angular velocity of the solid-body rotation of the vortex. The experimental law has been established for low magnetic Re_m: the experimental data points are represented by symbols. The convention used for these symbols is the same as in Fig. 3. The law of Roberts has been established for $Re_m \gg 1$. Consequently our global law for all the magnetic Reynolds numbers is probably not satisfactory around the point where the two laws cross, around $Re_m=2.7$. Elsewhere we can apply this law for estimations of the physical parameters of the Earth's core, supposing that thermal convection forms vortices in the Earth's core.

on the toroidal field from these analyses appears very weak: the kinematic dynamo of Pekeris *et al.* (1973) dissipates only 10^{-3} TW, with a toroidal field of 5 mT, while that of Kumar & Roberts (1975) dissipates 1.2 TW for a toroidal field of 200 mT. These dynamo models consider dissipation only at the largest (imposed) spatial scales of the velocity field. Our experiments suggest that this is not where most of the dissipation occurs. Instead, we find that dissipation by relatively small-diameter vertical vortices in the large-scale toroidal magnetic field could be predominant. The fact that the power spectrum of the poloidal field at the core–mantle boundary (Langel & Estes 1982; Hulot & Le Mouël 1994) is almost flat with harmonic degree l (beyond the dominant dipole), and hence that the spectrum of B^2 rises sharply with l (at least up to $l=13$), also point towards dominant dissipation at short scales.

We apply our scaling law for Joule heating of vertical vortices in a uniform horizontal magnetic field to estimate the upper bound on the toroidal magnetic field using two models for core flow, Busse's convection-driven dynamo and the 'observed' velocity field at the surface of the core. In the dynamo model of Busse (1970, 1975), thermal convection drives a circulation that takes the form of columnar vortices aligned with the axis of rotation (Taylor columns). The results of his analytical study indicate that the wavelength λ_c of this columnar instability in the equatorial plane is

$$\lambda_c = \left(\frac{Pr\sqrt{5/2}}{2E(1+Pr)}\right)^{1/3}, \qquad (31)$$

where Pr is the Prandtl number, and E the Ekman number. Taking for the Earth $Pr=1$ and $E=10^{-15}$, the number of columns is around 74 000. Assuming that these 6200 km high, narrow columns are arrayed within a uniform toroidal field B_T and that the magnetic Reynolds number of the columns does not exceed 1, we derive from eq. (25) and the upper bound (30) the fact that B_T cannot exceed 0.6 mT. It is probably not possible to sustain the geodynamo with such a low toroidal field, which indicates that the wavelength of convection deduced from Busse's analysis is too small for the core.

The second situation is perhaps more relevant, because it is based upon the observed velocity field. Maps of fluid velocity at the top of the core have been obtained from the analysis of the secular variation of the magnetic field (Gire & Le Mouël 1990; Bloxham *et al.* 1989; Jault 1990). We assume that the velocity field of Hulot, Le Mouël & Jault (1990), for example, is the surface expression of geostrophic vortices extending through the core. To estimate the amount of Joule heating produced by such geostrophic vortices, we assume their flow consists of four large-diameter vortices tangent to the inner core, with height = 5140 km, radius = 1135 km, and velocity = 5×10^{-4} m s^{-1}, plus four smaller equatorial vortices each with height = 4000 km, radius = 800 km, and velocity = 3×10^{-4} m s^{-1}. The Joule heating of this array in a uniform toroidal field B_T can be calculated with the aid of eq. (26). Using the upper bound (30), we find that B_T cannot exceed 9 mT for such a flow. Considering that we have

computed the highest possible dissipation, and that smaller-scale features have not been included, the toroidal magnetic field in the earth should be even smaller. On this basis, dynamo mechanisms that require a B_T/B_P ratio of more than about 20 are probably too dissipative for the Earth's core.

6 CONCLUSION

We have measured Joule dissipation in a vortex of liquid gallium permeated by a uniform transverse magnetic field, up to a magnetic Reynolds number of 0.3. The data indicate two regimes, which reflect the change in flow structure with increasing magnetic field intensity. For low magnetic field intensity the main effect of the Lorentz force is to reduce the fluid velocity while increasing the dimensions of the vortex. In this regime the Joule heating varies as the square of the imposed field. For very intense fields the Lorentz forces destroy the two-dimensionality of the vortex and the Joule heating becomes nearly independent of the applied field intensity or can decrease when B increases. Using the induced magnetic field to calibrate the actual velocity in the vortex, we find a simple scaling law for Joule heating P_J, with the form

$$P_J \simeq 4Re_m^2 P_D \tag{32}$$

in the first regime, where Re_m is the magnetic Reynolds number based on the fluid velocity and $P_D = H_{vortex} B^2/\mu_0^2\sigma$ is the Joule heating by magnetic diffusion (with no motion). We compared this result with the Joule heating predicted in the asymptotic limit of high Re_m using the flux-expulsion model of Roberts

$$P_J \simeq 18\sqrt{Re_m} P_D. \tag{33}$$

We applied these two formulas to estimate Ohmic dissipation of geostrophic vortices in the large-scale magnetic field inside the Earth's core. We find that large Joule heating occurs by this mechanism. This places some limitations on the intensity of magnetic fields allowed within the core, since the total Joule heat production within the core is limited thermodynamically. For example, using an upper bound of 0.5 TW for Joule heating in the core and the model of Hulot *et al.* (1990) for core vortices, we find that the toroidal magnetic field in the core cannot be larger than 9 mT (about 20 times the observed poloidal field). Although this upper bound is ample to explain the geodynamo, it is less than some dynamo models predict. This indicates that Joule heat production can be used to constrain models of the geodynamo.

ACKNOWLEDGMENTS

This study would not have taken place without the skilful technical assistance of Guy Marolleau. We are very much indebted to Rhône–Poulenc who lent us the gallium used in the experiments, thanks to the effort of H. Lauvray. We thank two anonymous reviewers for constructive remarks. We thank Ralph Holz and Caroline Dumoulin for helping with the experiments. The visit of Peter Olson was made possible through support from the École Normale Supérieure. This study is supported by CNRS-INSU, in particular through its program 'Terre Profonde'.

REFERENCES

Bloxham, J., Gubbins, D. & Jackson, A., 1989. Geomagnetic secular variation, *Phil. Trans. R. Soc. Lond.*, A, **329,** 415–502.

Braginski, S., 1990. Towards a realistic theory of the geodynamo, *Geophys. astrophys. Fluid Dyn.*, **60,** 89–134.

Brito, D., Cardin, P., Nataf, H.-C. & Marolleau, G., 1995. Experimental study of a geostrophic vortex of gallium in a transverse magnetic field, *Phys. Earth planet. Inter.*, **91,** 77–98.

Bullard, E.C. & Gellman, H., 1954. Homogeneous dynamos and terrestrial magnetism, *Phil. Trans. R. Soc. Lond.*, A, **247,** 213–278.

Busse, F.H., 1970. Thermal instabilities in rapidly rotating systems, *J. Fluid Mech.*, **44,** 441–460.

Busse, F.H., 1975. A model of the Geodynamo, *Geophys. J. R. astr. Soc.*, **42,** 437–459.

Cardin, P. & Olson, P., 1992. An experimental approach to thermo-chemical convection in the earth's core, *Geophys. Res. Lett.*, **19,** 1995–1998.

Cardin, P. & Olson, P., 1994. Chaotic thermal convection in a rapidly rotating spherical shell: consequences for flow in the outer core, *Phys. Earth planet. Inter.*, **82,** 235–259.

Elsasser, W., 1946. Induction effects in terrestrial magnetism 1: Theory, *Phys. Rev.*, **69,** 106–116.

Gire, C. & Le Mouël, J.-L., 1990. Tangentially geostrophic flow at the core mantle boundary compatible with the observed geomagnetic secular variation: the large scale component of the flow, *Phys. Earth planet. Inter.*, **59,** 259–287.

Glatzmaier, G.A. & Roberts, P.H., 1995. A three-dimensional convective dynamo solution with rotating and finitely conducting inner core and mantle, *Phys. Earth planet. Inter.*, **91,** 63–75.

Gubbins, D. & Roberts, P.H., 1987. Magnetohydrodynamics of the Earth's core, in *Geomagnetism,* Vol. 2, pp. 1–184, ed. Jacobs, J.A., Academic Press, London.

Gubbins, D., Masters, T.G. & Jacobs, J.A., 1979. Thermal evolution of the Earth's core, *Geophys. J. R. astr. Soc.*, **59,** 57–99.

Hulot, G. & Le Mouël, J.-L., 1994. A statistical approach to the Earth's main magnetic field, *Phys. Earth planet. Inter.*, **82,** 167–183.

Hulot, G., Le Mouël, J.-L. & Jault, D., 1990. The flow at the core–mantle boundary: symmetry properties, *J. Geomag. Geoelectr.*, **42,** 857–874.

Jault, D., 1990. Variations séculaires du champ géomagnétique et fluctuations de la longueur du jour, *Thèse de l'université Paris VII,* Paris, France.

Kumar, S. & Roberts, P.H., 1975. A three-dimensional kinematic dynamo, *Proc. R. Soc. Lond.*, A, **344,** 235–258.

Langel, R.A. & Estes, R.H., 1982. Geomagnetic field spectrum, *Geophys. Res. Lett.*, **9,** 250–253.

Lister, J.R. & Buffett, A., 1995. The strength and efficiency of thermal compositional convection in the geodynamo, *Phys. Earth planet. Inter.*, **91,** 17–30.

Loper, D.E. & Roberts, P.H., 1983. Compositional convection and the gravitationally powered dynamo, *Stellar and Planetary Magnetism,* Gordon & Breach, London.

Olson, P.L. & Glatzmaier, G.A., 1995. Magnetoconvection in a rotating spherical shell: structure of flow in the outer core, *Phys. Earth planet. Inter.*, **92,** 109–118.

Pascal, P., 1961. *Nouveau traité de chimie minérale VI,* Masson et Cie éditeurs, Paris, 669–774.

Pekeris, C.L., Accad, Y. & Shkoller, B., 1973. Kinematic dynamos and the Earth's magnetic field, *Phil. Trans. R. Soc. Lond.*, A, **275,** 425–461.

Tritton, D.J., 1988. *Physical Fluid Dynamics,* 2nd edn, Oxford Science Publications.

Verhoogen, J., 1980. *Energetics of the Earth,* National Academy of Sciences, Washington, DC.

Voorhies, C.V., 1986. Steady flows at the top of the core derived from geomagnetic field models, *J. geophys. Res.*, **91,** 12 444–12 466.

Zhang, K.K. & Fearn, D., 1993. How strong is the invisible component of the magnetic field in the Earth's core?, *Geophys. Res. Lett.*, **20,** 2083–2088.